

# Contact-Induced Static Fatigue of Annealed and Tempered Glass

P. CHANTIKUL, D. B. MARSHALL, and B. R. LAWN\*

Department of Applied Physics, School of Physics, The University of New South Wales, Kensington, New South Wales 2033, Australia

The role of environmentally assisted crack growth in the contact-induced strength degradation of brittle surfaces was studied. Indentation fracture mechanics, incorporating a standard crack-velocity function, are used to predict remaining strength as a function of contact load and duration. Strength tests on annealed and tempered glass disks, indented with a diamond pyramid or tungsten carbide sphere in a water environment, are in accord with the predicted degradation characteristics. The results indicate that fatigue effects are likely to be of only secondary importance in designing for maximum resistance to in-service contact damage.

## I. Introduction

BRITTLE solids have a strong tendency to strength-degrading surface damage when exposed to small, hard particles. Basically, particle contacts produce severe stress concentrations, the tensile components of which generate characteristic microcrack patterns.<sup>1,2</sup> A framework for classifying and analyzing these patterns is now well established, according to whether the contact is essentially elastic ("blunt" indenters) or plastic ("sharp" indenters)<sup>3</sup>: elastic contact generates the so-called Hertzian cone crack and plastic contact generates median (or radial) and lateral cracks. "Real" contacts involving irregular contacts fall somewhere between these two bounds.

Several workers<sup>4-10</sup> have analyzed the strength-degradation characteristics of brittle surfaces in a wide range of contact situations, e.g. blunt/sharp indenters, static/impact loadings, and annealed/tempered surfaces. However, in the interest of simplicity, all have dealt explicitly with fracture under conditions of purely mechanical equilibrium, which is justifiable in certain situations, e.g. inert environments, impulsive loadings, or low temperatures. But there are many practical situations in which contact events are sustained over extended periods, in corrosive surroundings and at moderate or high temperatures. Chemical forces then augment the mechanical forces which act to initiate and propagate the indentation cracks.<sup>11-15</sup> In view of the potentially catastrophic role of environmentally assisted crack growth in ceramic engineering systems,<sup>16</sup> it is reasonable to ask to what extent such kinetic effects might be expected to enhance contact-induced strength degradation.

This question is addressed in the present study. The particular case of "static fatigue" is singled out for explicit attention, although it is emphasized that the generality of the indentation fracture approach extends to any time-dependent load cycle. Glass/water is the chosen model material/environment crack system. Empirical crack velocity relations are incorporated into the fracture mechanics description to provide predictions of degraded strength as a function of contact time. The results suggest that fatigue effects are not a major consideration in designing against strength losses (mainly because of the high stability of indentation cracks) except perhaps in the initiation stages of fracture.

## II. Theoretical Strength/Time Characteristics

Consider the strength of a brittle component containing a dominant, contact-induced flaw of characteristic dimension  $c_\tau$ , where  $\tau$  denotes the duration of a load pulse of magnitude  $P_m$ . Figure 1

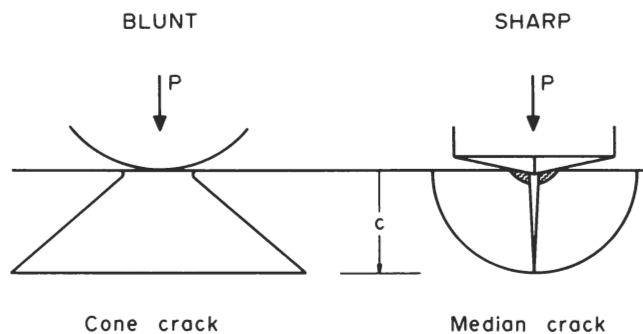


Fig. 1. Schematic of contact cracks;  $c$  denotes characteristic crack size at load  $P$  during indentation pulse.

indicates such a dimension for the two basic contact types. For simplicity, it is assumed that kinetic effects influence the crack growth only during the contact itself and not during the ensuing failure test used to determine remaining strength. Indentation fracture mechanics may then be applied readily to surfaces in the annealed or tempered state.

### (1) Annealed Surfaces

The standard relation for the strength of an indented brittle surface is

$$\sigma_\tau = K_c / (\pi \Omega_c c_\tau)^{1/2} \quad (\tau > 0) \quad (1)$$

where  $K_c$  is the critical stress intensity factor and  $\Omega_c$  is a dimensionless crack-geometry term conjugate to the indentation crack dimension  $c_\tau$ . In the limit of "instantaneous" contact this relation reduces to

$$\sigma_0 = K_c / (\pi \Omega_c c_0)^{1/2} \quad (\tau = 0) \quad (2)$$

corresponding to equilibrium fracture (ignoring stress-wave effects in the loading process). Then Eqs. (1) and (2) combine to give the time-dependent strength in reduced form,

$$\sigma_\tau = \sigma_0 (c_0 / c_\tau)^{1/2} \quad (c_\tau \geq c_0) \quad (3)$$

Indentation fracture mechanics may now be introduced to evaluate  $c_\tau$  and  $c_0$ . A complete analysis would involve consideration of both initiation and propagation of the contact cracks. The initiation stage is complex, especially when kinetic effects are present<sup>2,3,13</sup>; consequently, the observed environmentally induced reductions in threshold load  $P_c$  for cone- and median-crack formation are not easily quantified within a fracture mechanics framework. The propagation stage is relatively well understood, however; basically, the well-developed indentation fracture closely follows the mechanics of a center-loaded penny-like crack (Fig. 1), for which<sup>17</sup>

$$K = \chi P / c^{3/2} \quad (P > P_c) \quad (4)$$

is the stress intensity factor, with  $\chi$  a dimensionless indenter constant. The total response of an indentation crack over a full loading cycle may then be evaluated in accordance with an appropriate fracture criterion.

To establish a base for calculating fatigue characteristics it is necessary to consider first the prospective crack growth under mechanical equilibrium conditions,

$$K = K_c \quad (5)$$

If the maximum applied load does not exceed the threshold for initiation, i.e. if  $P_m < P_c$ , there can be no crack growth. However, if  $P_m > P_c$  the contact crack will initiate and extend stably with the load

Received January 24, 1978; revised copy received April 19, 1978.

Supported by the Australian Research Grants Committee. P. Chantikul's research was supported in part by a Commonwealth Government Grant under the Colombo Plan.

\*Member, the American Ceramic Society.

until, at maximum contact, it reaches its maximum size  $c_m$ : Eqs. (4) and (5) then give

$$c_m = (\chi P_m / K_c)^{2/3} \quad (P_m > P_c) \quad (6)$$

as the final size of the indentation flaw (assuming no healing during unloading), regardless of pulse shape.

Introducing kinetic effects gives rise to subcritical crack growth, governed by some crack velocity equation. For design purposes the crack velocity is most conveniently represented by an empirical power function,<sup>16</sup>

$$v_c = v_0 (K / K_c)^n \quad (K < K_c) \quad (7)$$

where  $v_0$  and  $n$  are material constants whose values must be determined by experimental calibration. In conjunction with Eq. (4), Eq. (7) may be integrated in the fully propagating region:

$$v_0 (\chi / K_c)^n \int_0^\tau [P(t)]^n dt = \int_{c_0}^{c_\tau} c^{3n/2} dc \quad (8)$$

Evaluation of this integral then requires the load pulse  $P(t)$  to be specified.

For the special case of static fatigue  $P(t)$  is of the form

$$\begin{aligned} P &= 0 & (t < 0) \\ P &= P_m & (0 \leq t \leq \tau) \\ P &= 0 & (t > \tau) \end{aligned} \quad (9)$$

Provided the threshold condition  $P_m > P_c$  is met in the limit of  $\tau \rightarrow 0$ , initial conditions for the integration may be determined from the equilibrium crack size in Eq. (6), i.e.  $c_0 = c_m$  at  $t = 0$ . Equation (8) then reduces to

$$c_\tau^{3n/2+1} - c_m^{3n/2+1} = (3n/2+1)(\chi P_m / K_c)^n v_0 \tau \quad (10)$$

Substituting Eqs. (10) and (6) into Eq. (3) finally gives the strength of the indented surface:

$$\sigma_\tau = \sigma_0 (1 + N \xi \tau / P_m^{2/3})^{-1/N} \quad (11)$$

where

$$\begin{aligned} N &= 3n + 2 \\ \xi &= 1/2 v_0 (K_c / \chi)^{2/3} \end{aligned} \quad (12)$$

are adjustable parameters determined by material toughness ( $K_c$ ), material/environment kinetic constants ( $n$  and  $v_0$ ), and indenter geometry ( $\chi$ ).

It is emphasized that Eq. (11) is derived on the assumption that crack formation occurs during initial indenter loading. If  $P_m < P_c$  at  $\tau \rightarrow 0$  the need to incorporate details of initiation mechanics into the integration formalism seriously complicates the problem. In such a case one may expect to observe an abrupt decrease in strength, corresponding to delayed formation of the indentation crack, as the contact time increases.

### (2) Tempered Surfaces

With tempered surfaces the procedure is basically the same as above. It is necessary only to modify some of the fracture mechanics equations to allow for a residual surface compressive stress  $\sigma_R$ .<sup>8</sup>

The strength of a tempered surface containing an indentation crack is, in analogy to Eqs. (1) and (2),

$$\sigma_\tau = K_c / (\pi \Omega_c c_\tau)^{1/2} + \sigma_R \quad (\tau > 0) \quad (13)$$

$$\sigma_0 = K_c / (\pi \Omega_c c_0)^{1/2} + \sigma_R \quad (\tau = 0) \quad (14)$$

Thus

$$\begin{aligned} \sigma_\tau = \sigma_0 (c_0 / c_\tau)^{1/2} [1 + (\pi \Omega_c c_\tau)^{1/2} \sigma_R / K_c] / \\ [1 + (\pi \Omega_c c_0)^{1/2} \sigma_R / K_c] \quad (c_\tau \geq c_0) \end{aligned} \quad (15)$$

With regard to the indentation fracture process, the residual compression acts as an inhibiting agent. Again it is only the propagation stage which is amenable to straightforward analysis; the modified form of Eq. (4) is

$$K = \chi P / c^{3/2} - \sigma_R (\pi \Omega_c c)^{1/2} \quad (P > P_c) \quad (16)$$

In equilibrium growth, as per Eq. (5), the conditions  $c = c_m$  at  $P = P_m$  corresponding to maximum contact give the propagation relation

$$K_c = \chi P_m / c_m^{3/2} - \sigma_R (\pi \Omega_c c_m)^{1/2} \quad (P_m > P_c) \quad (17)$$

from which the final size of the indentation flaw may be determined numerically.

Allowance for kinetic effects is made via integration of the crack velocity function Eq. (7), as before. In conjunction with Eqs. (9) and (16), the static fatigue equation for the indentation of tempered surfaces takes the form

$$v_0 (\chi P_m / K_c)^n \tau = \int_{c_0}^{c_\tau} c^{3n/2} dc / \{1 - (\pi \Omega_c)^{1/2} (\sigma_R / \chi P_m) c^2\}^n \quad (18)$$

which compares with Eq. (8). Adopting  $c_0 = c_m$  at  $t = 0$  once more as initial conditions, the integral may be solved numerically for the function  $c_\tau(\tau)$ . The strength  $\sigma_\tau(\tau)$  then follows from Eq. (15).

## III. Experimental Procedure and Results

### (1) Test Procedure

Optical quality glass disks, nominally 50 mm in diam. and 3 mm thick, were used as test specimens.<sup>8</sup> These disks were obtained commercially in the thermally tempered state,  $\sigma_R = (128 \pm 15)$  MPa, or the annealed state,  $\sigma_R = (0 \pm 2)$  MPa. The specimens were indented with either a Vickers diamond pyramid or a 1.58 mm radius tungsten carbide sphere. With the pyramidal indenter the specimen surfaces were tested in their as-received state,<sup>6</sup> whereas with the spherical indenter the prospective contact areas were preabraded with SiC grit<sup>5</sup>; sharp indenters are capable of producing their own starting flaws for crack growth, but blunt indenters require a suitable density of preexisting nucleation centers.<sup>3</sup> Equilibrium indentation tests were carried out in a dry nitrogen atmosphere, with a total contact time  $< 3$  s. Kinetic tests were carried out in a distilled water environment, with the prescribed load  $P_m$  held constant over time  $\tau$ ; the rise and fall times in the load pulse were  $\leq 1$  s. To avoid moisture effects in the remaining stage of the test sequence the newly indented surfaces were dried in warm air and the contact sites covered with a drop of paraffin oil. The disks were then loaded to rupture in a concentric ring-on-ring arrangement,<sup>8</sup> indented face in tension, to determine the degraded strength.

### (2) Results

Static fatigue functions  $[\sigma_\tau(\tau)]_{P_m}$  were investigated for both indenter types. At each prescribed set of indentation conditions, at least 10 specimens were broken (except at durations  $\tau > 5$  h, in which case the minimum number was 6) and the data were then reduced to a representative mean and standard deviation. Corresponding theoretical degradation functions were generated from the analysis of Section II, using the following constants for the glass/water system:  $K_c = (0.47 \pm 0.07)$  MPa  $m^{1/2}$ ,  $\chi = 0.057 \pm 0.011$  and  $\Omega_c = 0.41$  (Vickers indenter),  $\chi = (0.89 \pm 0.15) \times 10^{-3}$  and  $\Omega_c = 0.62$  (spherical indenter), as per calibration indentation/strength data<sup>8</sup>;  $n = 13.7$  and  $v_0 = 2.5$  mm  $s^{-1}$  from crack propagation data.<sup>15</sup> Instantaneous strengths  $\sigma_0$  for converting normalized stresses to absolute values were determined in one of two ways, recalling that the fatigue degradation theory assumes  $P_m > P_c$  at  $\tau \rightarrow 0$ : for loading conditions respecting this assumption,  $\sigma_0$  was most conveniently obtained from equilibrium indentation/strength data; where the assumption was violated, a conservative value for  $\sigma_0$  was determined consistent with  $c_0 = c_m$  by simultaneous solution of Eqs. (2) and (6) (or, for tempered surfaces, Eqs. (14) and (17)). In this context the equilibrium threshold loads for annealed surfaces were measured at  $P_c < 1$  N from indentations made with a pyramid on as-received surfaces and  $P_c = (195 \pm 27)$  N from indentations made with a sphere on preabraded surfaces. Figures 2 and 3 compare experimental results (data points) with the theoretical predictions (solid curves) determined in this way.

Figure 2 shows sharp-indenter fatigue behavior for both annealed and tempered specimens, at a contact load  $P_m = 100$  N, i.e.

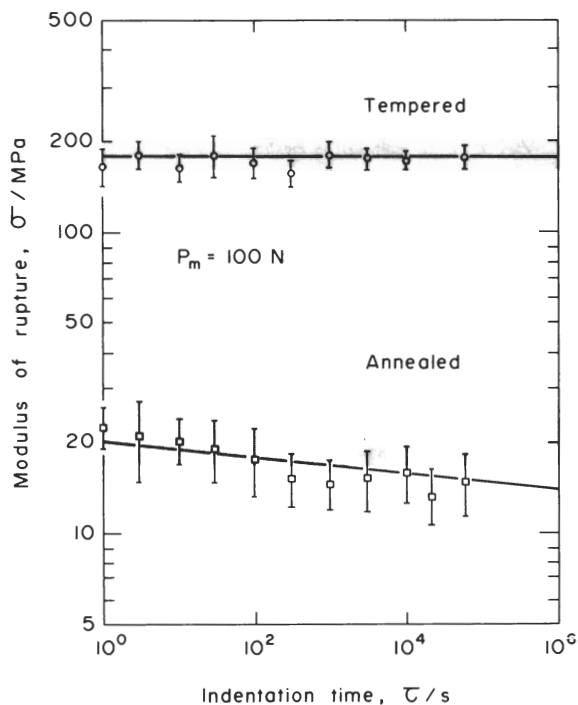


Fig. 2. Fatigue characteristics for Vickers pyramid indentation on annealed and tempered glass (as-received surfaces) in water. Shading designates measured limit of equilibrium strength.

well above threshold. The most noteworthy feature of these results is the small fatigue effect, particularly with the tempered surfaces.

Figure 3 shows blunt-indenter behavior for annealed specimens only, at contact loads  $P_m = 100$  N and 400 N, respectively, below and above threshold. At the higher load the results show the same trend as in Fig. 2. However, at the lower load there is an abrupt strength decrease due to the delayed cone-crack formation. Whereas the scale of this decrease depends critically on the size of preexisting surface flaws, the long-term strength universally approaches the curve computed on the basis of full crack propagation throughout the loading.

#### IV. Discussion

The results summarized in Figs. 2 and 3 indicate that fatigue effects will tend to manifest themselves more strongly in the initiation than in the propagation of strength-degrading contact fractures. This tendency relates to the stability characteristics of indentation cracks. The initiation stage is distinguished by an instability (threshold) in the crack evolution, corresponding to abrupt strength decrease in the manner of the data for  $P_m = 100$  N in Fig. 3. In such a situation the starting conditions for the indentation fracture might be expected to have some influence on the kinetics, since the accelerating flaw must spend most of its time close to its precontact configuration where growth is slowest. However, any such tendencies in the data shown at the bottom in Fig. 3 are obscured by the experimental scatter. Conversely, the propagation stage is characterized by highly stable growth in a rapidly diminishing long-range contact field, as reflected in the steady decline in the long-term strength. Starting conditions become a minor consideration (provided, of course, that a flaw does exist for threshold to occur), the decelerating crack now spending most of its time close to its final configuration, causing the rapid convergence of both sets of data to the computed curve for  $P_m = 100$  N in Fig. 3. The existence of a fatigue limit in the crack propagation must ultimately establish a lower bound to the strength degradation for any given set of contact conditions.

It is interesting to note the extreme resistance to fatigue effects shown by tempered surfaces (Fig. 2). Detailed analysis of the fracture mechanics<sup>18</sup> explains this behavior in terms of the action of

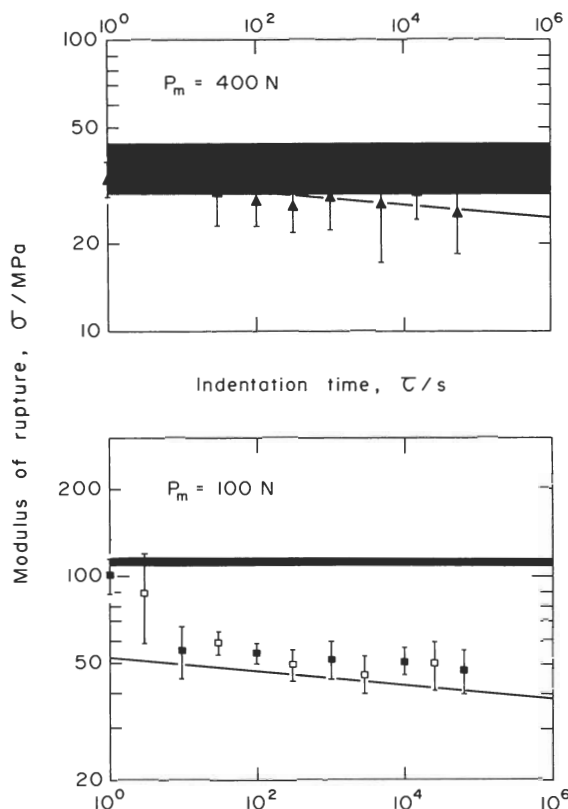


Fig. 3. Fatigue characteristics for sphere indentation on annealed glass (preabraded surfaces) in water. Filled symbols and heavy shading indicate abrasion with 400-mesh SiC grit blast, open symbols and light shading abrasion with 150-mesh SiC grit free fall through 0.5 m.

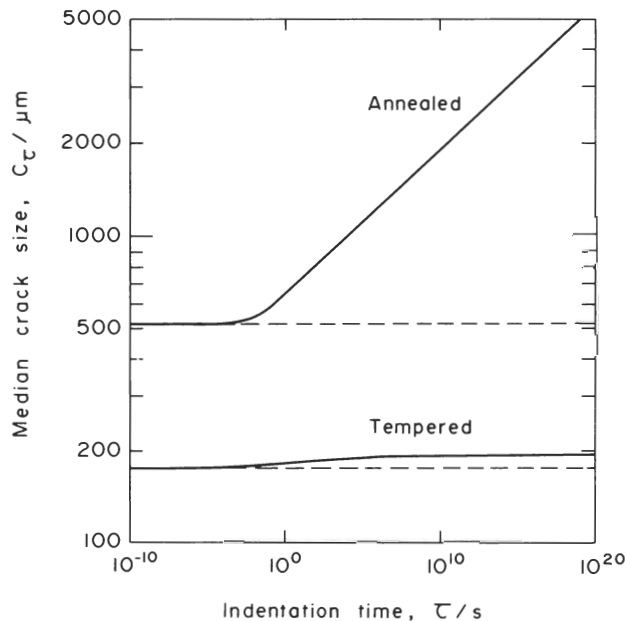


Fig. 4. Computed crack size as a function of indentation time for Vickers pyramid on annealed and tempered glass in water;  $P_m = 100$  N. Curves evaluated appropriate to indentation conditions of Fig. 2.

residual compression stresses in opposing crack extension; the range of crack lengths over which the net driving force on the crack is actually positive (i.e.  $K > 0$ ) in fixed-load indentation is accordingly restricted. This restriction is evident in Fig. 4, showing comparative  $c_\tau(\tau)$  functions for tempered surfaces from Eqs. (18) and (17) and for annealed surfaces from Eqs. (10) and (6). Surface

tempering would therefore appear to offer especially high immunity to strength losses in those service environments where corrosive elements assist in the activation of mechanical damage processes. (However, these advantages are all lost if the contact-induced fracture penetrates beyond the near-compression region and into the inner tension zone of the tempered plate, where failure occurs spontaneously.<sup>8,18</sup>)

In the present study an analysis has been made of one special case of time-dependent loading, that of "static fatigue," as defined by Eq. (9). There is nothing in the formulation to prevent extension of the analysis to more general load functions  $P(t)$ : "Dynamic fatigue," where load rate  $\dot{P}$ , rather than  $P_m$ , is maintained constant in magnitude, is one important example.

## References

- <sup>1</sup> F. C. Frank and B. R. Lawn, "Theory of Hertzian Fracture," *Proc. R. Soc. London, Ser. A*, **299** [1458] 291-306 (1967).
- <sup>2</sup> B. R. Lawn and M. V. Swain, "Microfracture Beneath Point Indentations in Brittle Solids," *J. Mater. Sci.*, **10** [1] 113-22 (1975).
- <sup>3</sup> B. R. Lawn and T. R. Wilshaw, "Indentation Fracture: Principles and Applications," *J. Mater. Sci.*, **10** [6] 1049-81 (1975).
- <sup>4</sup> A. G. Evans, "Strength Degradation by Projectile Impacts," *J. Am. Ceram. Soc.*, **56** [8] 405-409 (1973).
- <sup>5</sup> B. R. Lawn, S. M. Wiederhorn, and H. H. Johnson, "Strength Degradation of Brittle Surfaces: Sharp Indenters," *ibid.*, **59** [5-6] 193-97 (1976).
- <sup>6</sup> B. R. Lawn, E. R. Fuller, and S. M. Wiederhorn, "Strength Degradation of Brittle Surfaces: Sharp Indenters," *ibid.*, **59** [5-6] 193-97 (1976).
- <sup>7</sup> S. M. Wiederhorn and B. R. Lawn, "Strength Degradation of Glass Resulting from Impact with Spheres," *ibid.*, **60** [9-10] 451-58 (1977).
- <sup>8</sup> D. B. Marshall and B. R. Lawn, "Strength Degradation of Thermally Tempered Glass Plates," *ibid.*, **61** [1-2] 21-27 (1978).
- <sup>9</sup> S. M. Wiederhorn and B. R. Lawn, "Strength Degradation of Glass Impacted with Sharp Particles: I"; to be published in the *Journal of the American Ceramic Society*.
- <sup>10</sup> B. R. Lawn, D. B. Marshall and S. M. Wiederhorn, "Strength Degradation of Glass Impacted with Sharp Particles: II"; to be published in the *Journal of the American Ceramic Society*.
- <sup>11</sup> F. C. Roesler, "Brittle Fractures Near Equilibrium," *Proc. Phys. Soc., London, Sect. B*, **69** [10] 981-92 (1956).
- <sup>12</sup> C. J. Culf, "Fracture of Glass Under Various Liquids and Gases," *J. Soc. Glass Technol.*, **41** [199] 157-67T (1957).
- <sup>13</sup> F. B. Langitan and B. R. Lawn, "Effect of a Reactive Environment on the Hertzian Strength of Brittle Solids," *J. Appl. Phys.*, **41** [8] 3357-65 (1970).
- <sup>14</sup> A. G. Mikosza and B. R. Lawn, "Section-and-Etch Study of Hertzian Fracture Mechanics," *J. Appl. Phys.*, **42** [13] 5540-45 (1971).
- <sup>15</sup> M. V. Swain and B. R. Lawn, "Microprobe Technique for Measuring Slow Crack Velocities in Brittle Solids," *Int. J. Fract.*, **9** [4] 481-83 (1973).
- <sup>16</sup> S. M. Wiederhorn, pp. 633-63 in *Ceramics for High Performance Applications*. Edited by J. J. Burke, A. E. Gorum, and R. N. Katz. Brook Hill, Chestnut Hill, Mass., 1974.
- <sup>17</sup> B. R. Lawn and E. R. Fuller, "Equilibrium Penny-Like Cracks in Indentation Fracture," *J. Mater. Sci.*, **10** [12] 2016-24 (1975).
- <sup>18</sup> B. R. Lawn and D. B. Marshall, "Contact Fracture Resistance of Physically and Chemically Tempered Glass Plates: A Theoretical Model," *Phys. Chem. Glasses*, **18** [1] 7-18 (1977).